Stratospheric winter climate response to ENSO in three chemistry-climate models

A. M. Fischer,[1] D. T. Shindell,[2] B. Winter,[3] M. S. Bourqui,[3] G. Faluvegi,[2] E. Rozanov,[1,4] M. Schraner,[1] and S. Brönnimann[1]

Received 10 April 2008; accepted 3 June 2008; published 11 July 2008.

[1] Three different chemistry-climate models are compared with respect to their simulation of the stratospheric response to extreme cases of ENSO. Ensemble simulations of an unusually warm ENSO event (1940–1941) compared to a very cold event (1975–1976) reveal a weaker and warmer polar vortex in the Northern Hemisphere winter. This follows from anomalously propagating waves decelerating the zonal flow and strengthening the residual mean circulation. Models are in good agreement in simulating the observed (statistically reconstructed for the case 1941) flow in the lower stratosphere over the Pacific North American region, but less so over the North Atlantic European sector with insufficient reproduction of the wave structure. Modeled column ozone is reduced in the Tropics and increased on average in the northern extra tropics in accord with the general pattern seen in observations and in line with an intensification of the Brewer-Dobson circulation. **Citation:** Fischer, A. M., D. T. Shindell, B. Winter, M. S. Bourqui, G. Faluvegi, E. Rozanov, M. Schraner, and S. Brönnimann (2008), Stratospheric winter climate response to ENSO in three chemistry-climate models, *Geophys. Res. Lett.*, *35*, L13819, doi:10.1029/2008GL034289.

1. Introduction

[2] El Niño-Southern Oscillation (ENSO) is an important driver for modulating the stratospheric climate in the Northern Hemisphere (NH) on an interannual timescale. Observational studies revealed that warm ENSO (wENSO) events are associated with a weak and warm polar vortex over the Arctic during boreal wintertime [*Van Loon and Labitzke*, 1987]. Using models with sufficiently high vertical resolution it can be shown that ENSO is affecting the northern winter polar vortex by anomalously vertical propagating waves, thereby increasing wave mean flow interaction and the residual mean circulation (RMC) resulting in a colder (warmer) tropical (mid-latitudinal) stratosphere [*Brönnimann et al.*, 2004; *García-Herrera et al.*, 2006; *Manzini et al.*, 2006; *Sassi et al.*, 2004; *Taguchi and Hartmann*, 2006]. Disentangling the ENSO signal on the Northern stratospheric climate from other perturbing factors (i.e. solar activity, QBO phase, stratospheric aerosol loading) is a particularly difficult task when analyzing transient chemistry-climate model (CCM) simulations as well as observational data [*Camp and Tung*, 2007]. Studying the atmospheric response to a single ENSO cycle as in the work by *Brönnimann et al.* [2006], requires comparable forcing conditions for both phases, wENSO and cold ENSO (cENSO), which occurs only rarely. Here we present a model intercomparison of an unusual wENSO event from 1939–1942 [*Brönnimann et al.*, 2004] with respect to a strong cENSO event from 1975–1976. A CCM simulation reproducing this extreme case not only leads to a better understanding on the processes prevailing but also serves as an insightful model test with respect to the communication of the ENSO signal, the propagation of planetary waves and the response in stratospheric ozone. The analysis involves three CCMs whose applicability lies in multi-decadal to centennial simulations or large ensemble sizes and which thus feature a coarser model grid than other state-of-the-art CCMs [see *Eyring et al.*, 2006]. The focus of this paper is restricted to the effect of stratospheric climate and dynamics in the NH during boreal winter.

2. Methods

[3] The model intercomparison comprises the CCMs SOCOL (based on work by *Egorova et al.* [2005]), G-PUCCINI [*Shindell et al.*, 2006] and IGCM-FASTOC [*Taylor and Bourqui*, 2005]. The horizontal resolution in SOCOL and IGCM-FASTOC is similar (about 3.75°) and slightly higher than in G-PUCCINI (4° × 5°). In the vertical SOCOL has a resolution of 39 layers from the surface up to 0.01 hPa. This is higher than the vertical representation in G-PUCCINI (23 layers up to 0.01 hPa) and IGCM-FASTOC (26 layers up to 0.1 hPa) (Table 1; see the online supporting material for detailed information about these models).

[4] The models were run from July 1940 until July 1941 (wENSO) and July 1975 until July 1976 (cENSO), and the analysis focuses on the respective late winter periods (1941, 1976). The simulations were performed in ensemble mode with 20 members in SOCOL and G-PUCCINI and 50 members in IGCM-FASTOC. The statistical significance of the simulated winter difference is calculated using Student's t-test.

[5] For forcing SOCOL and G-PUCCINI we used monthly varying sea surface temperature [*Smith and Reynolds*, 2004] and sea ice distribution [*Rayner et al.*, 2003]. IGCM-FASTOC was forced at the surface by monthly averaged surface air temperatures from an ensemble mean simulation using SOCOL in order to

[1]Institute for Atmospheric and Climate Science, ETH Zurich, Zurich, Switzerland.
[2]NASA Goddard Institute for Space Studies, New York, New York, USA.
[3]Department of Atmospheric and Oceanic Sciences, McGill University, Montréal, Québec, Canada.
[4]Physical-Meteorological Observatory/World Radiation Center, Davos, Switzerland.

Copyright 2008 by the American Geophysical Union.
0094-8276/08/2008GL034289

Table 1. Overview of the Model Resolution, Ensemble Size and the Considered External Forcings[a]

Model	Resolution/Top	Ensemble Size	Forcings
SOCOL	T30L39/0.01 hPa	20	SST/SI, Solar, GHG, ODS, strataer
G-PUCCINI	4° × 5°L23/0.01 hPa	20	SST/SI, Solar, GHG, ODS, strataer
IGCM-FASTOC	T31L26/0.1 hPa	50	SAT, GHG

[a]SST: Sea surface temperature, SI: Sea ice distribution, GHG: Greenhouse gases, ODS: Ozone depleting substances, strataer: stratospheric aerosols, Solar: total solar irradiance, SAT: Surface Air Temperature of the SOCOL ensemble mean simulation.

correctly simulate wave propagation. Changes in total solar irradiance were specified following *Lean* [2000] and for stratospheric aerosol loading we used compilations by *Sato et al.* [1993]. Both simulation periods were at solar minimum conditions and very similar in absolute terms. The aerosol loading in the stratosphere was low in both events but somewhat higher during 1975/1976 than 1940/1941.

[6] The CCM results are compared to several observational and reconstructed data products. For geopotential height (GPH) and temperature fields in the stratosphere in 1941 we used statistical reconstructions that are based on upper-level data [*Brönnimann and Luterbacher*, 2004]. The fields for 1976 are obtained from the ERA-40 re-analysis data [*Uppala et al.*, 2005]. We compared the signal in Total Ozone (TOZ) using several TOZ series in the NH, obtained from the World Ozone and Ultraviolet Radiation Data Centre (WOUDC).

3. Results

[7] Figure 1 displays winter difference, 1941–1976, of 100 hPa GPH and temperature averaged over January to March. This is the time when largest ENSO anomalies are observed in the lower stratosphere due to downward propagation from higher altitudes [see *Manzini et al.*, 2006]. The difference between reconstructions and ERA40 (referred to as "recERA") reveals elevated pressure over the Arctic region and over low latitudes and thus a weakening of the polar vortex accompanied by anomalous warm temperatures in line with previous modeling and observational studies [*Brönnimann et al.*, 2004; *García-Herrera et al.*, 2006; *Manzini et al.*, 2006; *Sassi et al.*, 2004; *Van Loon and Labitzke*, 1987]. The increase in temperature is zonally symmetric at northernmost latitudes and the magnitude of the signal is comparable to the results by *Sassi et al.* [2004] for February. Similar to *Manzini et al.* [2006] (for ERA-40), at mid-latitudes, a wave 2 component can be found with strong negative GPH anomaly centres over the Northern Pacific and Central Europe. In the Tropics a negative temperature anomaly stretches northwards over the Atlantic towards Asia.

[8] In general CCM results of the ensemble mean are in reasonable agreement with these patterns, though the magnitude is less strong. Unlike G-PUCCINI the internal variability of SOCOL and IGCM-FASTOC is quite large and some of its members capture the strong response in GPH and temperature as observed (see Figure S1, online supplementary material[1]). In the ensemble mean the models show a significant increase in tropical GPH together with the well-known positive (negative) dipole structure over the Eastern Tropical Pacific in GPH (temperature) [*Claud et al.*, 1999]. Note, that IGCM-FASTOC was forced with surface temperatures of SOCOL. In SOCOL, the weaker polar vortex during wENSO is manifest over the whole Arctic region, in contrast to IGCM-FASTOC and G-PUCCINI where it is restricted to the region west of Greenland. It is also interesting to note that the negative temperature anomaly band over tropical Pacific, Atlantic, North Africa and East Asia is very well reproduced by all CCMs. At mid-latitudes the wave imprint in GPH and temperature over the Pacific North American region is in remarkably good agreement with recERA, but the models diverge in correctly simulating the wave structure over the North Atlantic European sector. The observed GPH anomaly over Central Europe is shifted westward in SOCOL and G-PUCCINI and northward in IGCM-FASTOC (though not significantly), accompanied by a GPH increase over the Mediterranean and Europe. This mismatch is most probably caused by insufficient planetary wave propagation characteristics due to coarse model resolutions. Applying the same ENSO experiment with IGCM-FASTOC at a resolution of T21 instead of T31 resulted in a complete failure in reproducing any of the aforementioned characteristics (not shown). This emphasizes the importance of the horizontal model resolution in correctly reproducing the wave patterns in the NH during an ENSO cycle [see also *Merkel and Latif*, 2002].

[9] Several TOZ series are available in the NH for either the 1940s or 1970s, but only two for both periods. Therefore, the best way to compare the TOZ series during these events is by analyzing (smoothed) standardized anomalies with respect to a 7 yr time window surrounding each event [see *Brönnimann et al.*, 2004]. Figure 2 reveals that in the 1940s (1970s) strong positive (negative) anomalies are observed at all sites.

[10] For the winter difference between wENSO and cENSO all three CCMs exhibit a negative response over the Tropics (strongest over Pacific), which is, zonally averaged, of similar magnitude in SOCOL and G-PUCCINI and stronger than in IGCM-FASTOC. The signal north of 30°N becomes less clear due to a large ensemble spread in G-PUCCINI and IGCM-FASTOC (only the TOZ increase in response to the deepening of the Aleutian Low is significant in all models), but displays, zonally averaged, elevated TOZ over mid- to high latitudes in the ensemble means. In SOCOL this increase is a significant dominant signal over the whole Polar region covering the northernmost European TOZ stations. Note that the rather different responses at high latitudes in G-PUCCINI and in IGCM-FASTOC (particularly the negative anomalies over Alaska and Northern Europe) are not significant. It is interesting to note that a positive signal over East China and the southern tip of Japan (compare stations Shanghai and Tateno) as well as over the Northeast of the US (compare New York and Caribou) can be found in some of the models. This increase

[1]Auxiliary materials are available in the HTML. doi:10.1029/2008GL034289.

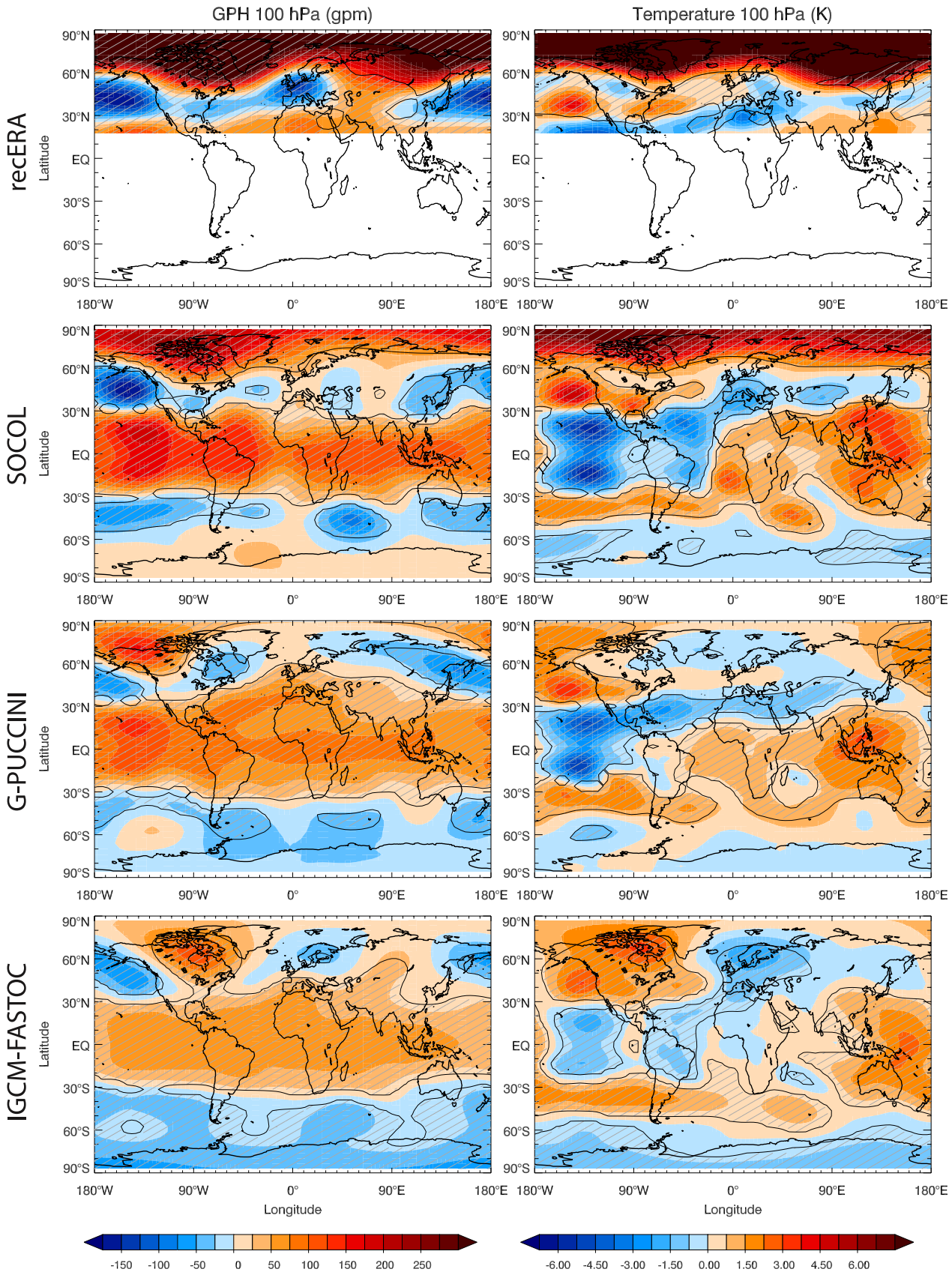

Figure 1. Difference between 1941 and 1976 in (left) GPH (in m) and (right) temperature (in K) at 100 hPa, averaged from January to March, for (top to bottom) recERA and SOCOL, G-PUCCINI and IGCM-FASTOC. Shaded areas together with contour lines in the bottom three plots mark statistically significant areas (t-test, p-value < 0.05). Shading with lines in the top plots denotes a high reconstruction skill (reduction of error > 0.2).

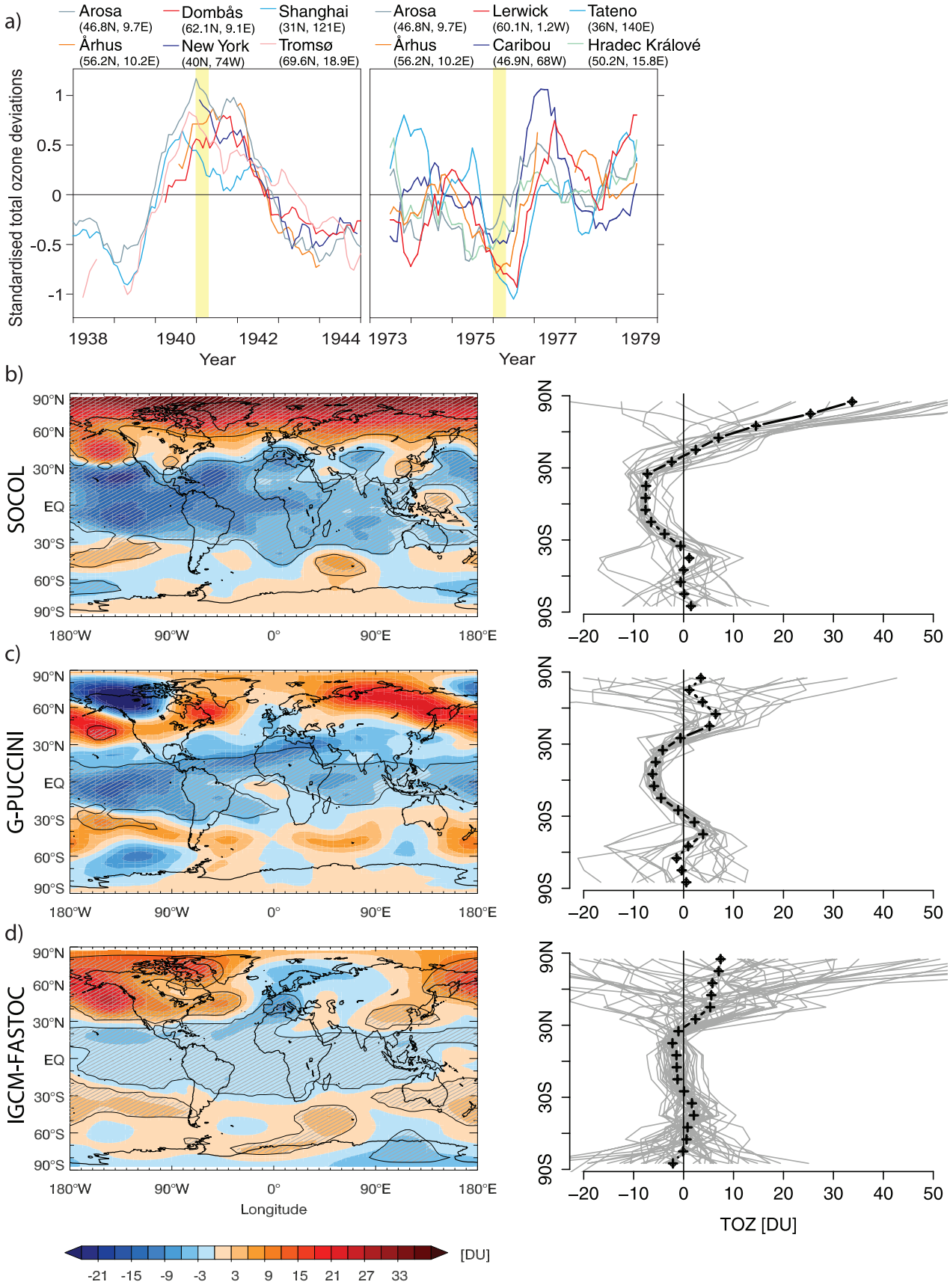
a)
Arosa (46.8N, 9.7E)
Dombås (62.1N, 9.1E)
Shanghai (31N, 121E)
Arosa (46.8N, 9.7E)
Lerwick (60.1N, 1.2W)
Tateno (36N, 140E)
Århus (56.2N, 10.2E)
New York (40N, 74W)
Tromsø (69.6N, 18.9E)
Århus (56.2N, 10.2E)
Caribou (46.9N, 68W)
Hradec Králové (50.2N, 15.8E)
Standardised total ozone deviations
Year
Year
b)
SOCOL
c)
G-PUCCINI
d)
IGCM-FASTOC
Longitude
TOZ [DU]
[DU]

Figure 2

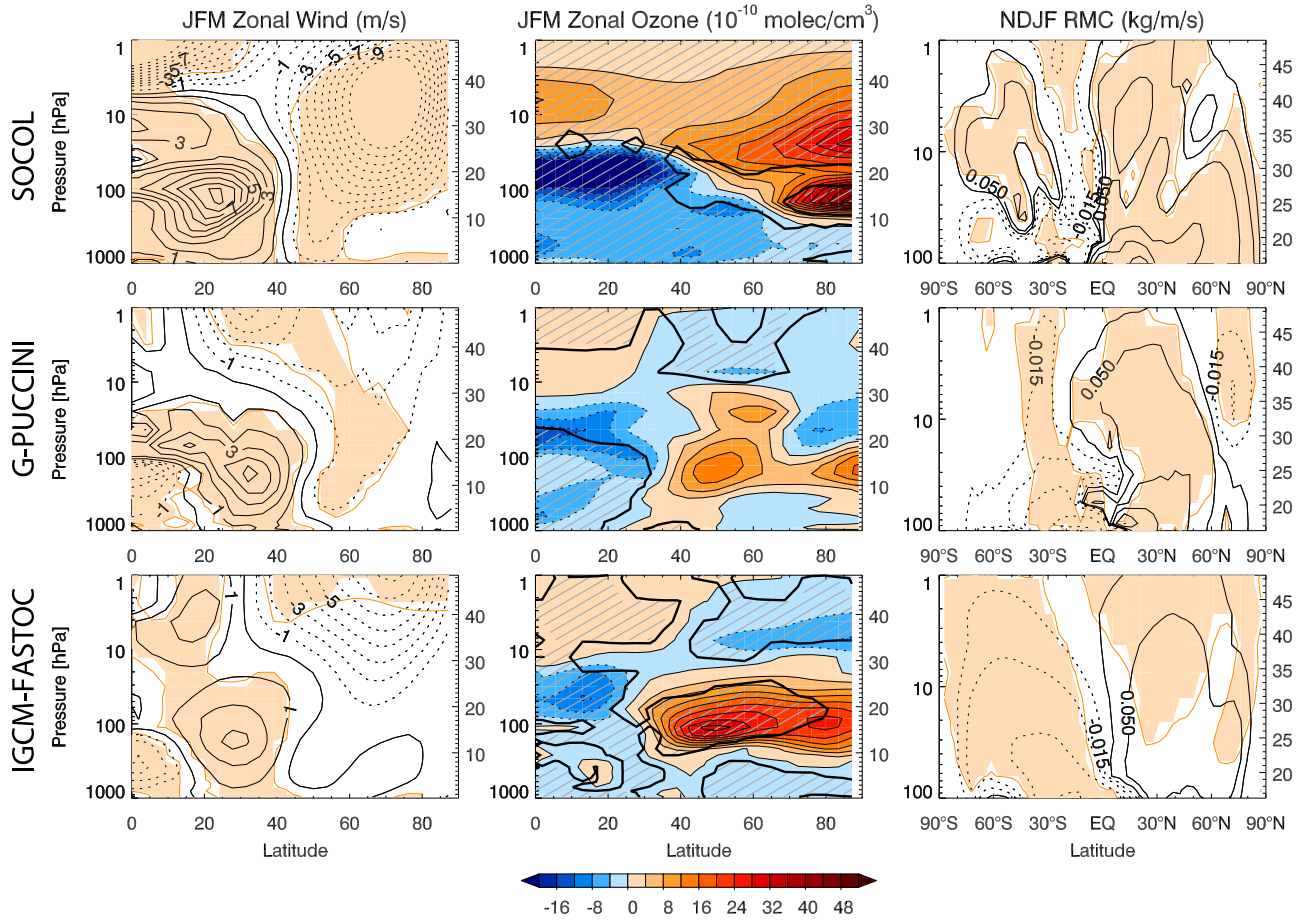

Figure 3. NH difference between 1941 and 1976 in (left) zonal mean zonal wind (in m/s), (middle) zonal mean ozone number densities (in 10^{-10} molecules/cm^3), and (right) RMC (in kg/m/s), averaged from (left and middle) January to March and (right) November to February, for (top) SOCOL, (middle) G-PUCCINI, and (bottom) IGCM-FASTOC. Shaded areas together with contour lines (orange on the left and right) mark statistically significant areas (t-test, p-value < 0.05).

was also observed in satellite data, described in a similar ENSO study [see *Brönnimann et al.*, 2006]. Agreement between model responses and TOZ stations, however, is poor for Central Europe which is possibly linked to the misrepresentation of the wave structure in this region.

[11] To elucidate dynamical and chemical changes, we have analyzed zonal mean zonal wind, ozone and RMC (see Figure 3). All CCMs show a significantly reduced zonal wind speed at polar latitudes, underlining the pattern of large-scale circulation anomalies at polar regions. At most, zonal flow is decelerated by more than 15 m/s (in SOCOL) at around 10 hPa. Similar to *Manzini et al.* [2006] we found that the decrease in wind speed proceeds to tropospheric layers in the mid-latitudes and thus directly affects climate at the ground. A strengthening of the subtropical jet is apparent in all models, but displaced southwards in SOCOL [see also *Brönnimann et al.*, 2006].

[12] Ozone in the equatorial lower stratosphere is significantly reduced in all CCMs resulting in the TOZ decrease in the Tropics seen above. Further northward at the same altitude ozone concentration is much enhanced in the response of all models (in G-PUCCINI not significantly). The response at higher altitudes is weaker and reverses in IGCM-FASTOC and G-PUCCINI. SOCOL simulates enhanced ozone throughout the NH with strongest changes at northernmost latitudes. The pattern of reduced ozone over the Tropics together with increased ozone and weakened zonal flow at higher latitudes in the stratosphere suggests a strengthening of the RMC, caused by anomalously vertical propagating waves [e.g., *García-Herrera et al.*, 2006]. The RMC difference, averaged over November to February,

Figure 2. (a) TOZ deviations from a climatology derived from the displayed time window for several stations in the NH (standardized for each station and smoothed with a 12-month moving average [*Brönnimann et al.*, 2004]) for (left) 1938–1944 and (right) 1973–1979. Yellow shading marks the analysed winter. (b–d) Difference between 1941 and 1976 TOZ (in DU), averaged from January to March, for ensemble mean field (left, shaded areas together with contour lines mark statistically significant areas, t-test, p-value < 0.05) and zonally averaged ensemble members (right in gray, ensemble mean in black and plus symbols) in SOCOL, G-PUCCINI and IGCM-FASTOC (all interpolated to 10° bins).

and thus accounting for possible time lags, shows an enhancement throughout the stratosphere in the NH, which increases the transport of ozone from the source region in the Tropics towards higher latitudes where the lifetime is considerably longer. EP flux divergence reveals a more convergent pattern in large part of the middle and upper stratosphere and a strengthening of the convergence zone at around 500 hPa resulting from both vertical and horizontal component (see Figure S2, online supplementary material). This result gives evidence of increased wave mean flow interaction eventually weakening the zonal flow and driving the RMC in all three CCMs.

4. Conclusion

[13] The presented models participating in this intercomparison are in reasonable agreement with recERA as well as previous model and observational studies of the ENSO imprint on stratospheric chemistry and climate. The detected main responses (acceleration of the RMC, weakening of the polar vortex, enhanced Equator to Pole transport of ozone) are most pronounced in SOCOL which has the highest resolution in the vertical. At mid- to high latitudes, within model variability for TOZ in IGCM-FASTOC and G-PUCCINI is large whereas for GPH and temperature the spread of ensemble members differs among the models but the bulk of it shows a weaker signal than in recERA. Over the Pacific North American sector agreement between the ensemble means and recERA is very promising, but less so over the North Atlantic European sector with respect to the wave pattern. The rather low horizontal resolution could explain some of the discrepancies. *Merkel and Latif* [2002] showed that increasing the horizontal model resolution can improve the reproduction of eddy-mean flow interaction over this region. Yet, the presented models are designed and used for multi-decadal and longer simulations, and thus have a grid resolution imposed by computational costs. For the application of long-term simulations we conclude that the presented models are suitable for capturing ENSO variability in the NH stratosphere given a sufficiently large set of ensemble simulations. Reproducing correctly strong SST-forced signals is a prerequisite for analyzing externally forced signals in CCMs. Note that by setting up this case study we have isolated the effect of ENSO from other potential sources of stratospheric variability (i.e. QBO, solar variability, volcanic eruptions). Thus, in a transient long-term simulation and corresponding composite study we expect the ENSO signal to be much less distinct. It may also be weaker during other ENSO cycles [e.g. *Brönnimann et al.*, 2006], as we have chosen here two extreme cases of ENSO. The variability calls for a large number of ensemble simulations when detecting and attributing ENSO effects on NH stratospheric climate in transient CCM simulations.

[14] **Acknowledgments.** A.F. is funded by ETH Zurich (TH project CASTRO) and S.B. by the Swiss National Science Foundation. We are grateful for valuable comments by Thomas Peter (IACETH). M.B. and B.W. are grateful to Chris Bell, University of Reading, UK, who updated the IGCM to the T31 resolution, and to the Canadian Foundation for Innovation and Recherche Québec for financing the computing infrastructure used in this study. B.W. was funded by the Canadian Foundation for Climate and Atmospheric Sciences. D.S. and G.F. acknowledge support from NASA's ACMAP. We thank WOUDC for providing TOZ station data. ERA-40 data have been obtained by ECMWF.

References

Brönnimann, S., and J. Luterbacher (2004), Reconstructing Northern Hemisphere upper-level fields during World War II, *Clim. Dyn.*, *22*, 499–510.

Brönnimann, S., J. Luterbacher, J. Staehelin, T. M. Svendby, G. Hansen, and T. Svenoe (2004), Extreme climate of the global troposphere and stratosphere in 1940–42 related to El Niño, *Nature*, *431*, 971–974.

Brönnimann, S., M. Schraner, B. Müller, A. Fischer, D. Brunner, E. Rozanov, and T. Egorova (2006), The 1986–1989 ENSO cycle in a chemical climate model, *Atmos. Chem. Phys.*, *6*, 4669–4685.

Camp, C. D., and K.-K. Tung (2007), Stratospheric polar warming by ENSO in winter: A statistical study, *Geophys. Res. Lett.*, *34*, L04809, doi:10.1029/2006GL028521.

Claud, C., N. A. Scott, and A. Chedin (1999), Seasonal, interannual, and zonal temperature variability of the tropical stratosphere based on TOVS satellite data: 1987–91, *J. Clim.*, *12*, 540–550.

Egorova, T., E. Rozanov, V. Zubov, E. Manzini, W. Schmutz, and T. Peter (2005), Chemistry-climate model SOCOL: A validation of the present-day climatology, *Atmos. Chem. Phys.*, *5*, 1557–1576.

Eyring, V., et al. (2006), Assessment of temperature, trace species, and ozone in chemistry-climate model simulations of the recent past, *J. Geophys. Res.*, *111*, D22308, doi:10.1029/2006JD007327.

García-Herrera, R., N. Calvo, R. R. Garcia, and M. A. Giorgetta (2006), Propagation of ENSO temperature signals into the middle atmosphere: A comparison of two general circulation models and ERA-40 reanalysis data, *J. Geophys. Res.*, *111*, D06101, doi:10.1029/2005JD006061.

Lean, J. (2000), Evolution of the Sun's spectral irradiance since the Maunder Minimum, *Geophys. Res. Lett.*, *27*, 2425–2428.

Manzini, E., M. A. Giorgetta, M. Esch, L. Kornblueh, and E. Roeckner (2006), The influence of sea surface temperatures on the northern winter stratosphere: Ensemble simulations with the MAECHAM5 model, *J. Clim.*, *19*, 3863–3881.

Merkel, U., and M. Latif (2002), A high resolution AGCM study of the El Niño impact on the North Atlantic/European sector, *Geophys. Res. Lett.*, *29*(9), 1291, doi:10.1029/2001GL013726.

Rayner, N. A., D. E. Parker, E. B. Horton, C. K. Folland, L. V. Alexander, D. P. Rowell, E. C. Kent, and A. Kaplan (2003), Global analyses of sea surface temperature, sea ice, and night marine air temperature since the late nineteenth century, *J. Geophys. Res.*, *108*(D14), 4407, doi:10.1029/2002JD002670.

Sassi, F., D. Kinnison, B. A. Boville, R. R. Garcia, and R. Roble (2004), Effect of El Niño–Southern Oscillation on the dynamical, thermal, and chemical structure of the middle atmosphere, *J. Geophys. Res.*, *109*, D17108, doi:10.1029/2003JD004434.

Sato, M., J. E. Hansen, M. P. Mccormick, and J. B. Pollack (1993), Stratospheric aerosol optical depths, 1850–1990, *J. Geophys. Res.*, *98*, 22,987–22,994.

Shindell, D. T., G. Faluvegi, N. Unger, E. Aguilar, G. A. Schmidt, D. M. Koch, S. E. Bauer, and R. L. Miller (2006), Simulations of preindustrial, present-day, and 2100 conditions in the NASA GISS composition and climate model G-PUCCINI, *Atmos. Chem. Phys.*, *6*, 4427–4459.

Smith, T. M., and R. W. Reynolds (2004), Improved extended reconstruction of SST (1854–1997), *J. Clim.*, *17*, 2466–2477.

Taguchi, M., and D. L. Hartmann (2006), Increased occurrence of stratospheric sudden warmings during El Niño as simulated by WACCM, *J. Clim.*, *19*, 324–332.

Taylor, C. P., and M. S. Bourqui (2005), A new fast stratospheric ozone chemistry scheme in an intermediate general-circulation model. I: Description and evaluation, *Q. J. R. Meteorol. Soc.*, *131*, 2225–2242.

Uppala, S. M., et al. (2005), The ERA-40 re-analysis, *Q. J. R. Meteorol. Soc.*, *131*, 2961–3012.

Van Loon, H., and K. Labitzke (1987), The Southern Oscillation. Part V: The anomalies in the lower stratosphere of the Northern Hemisphere in winter and a comparison with the Quasi-Biennial Oscillation, *Mon. Weather Rev.*, *115*, 357–369.

M. S. Bourqui and B. Winter, Department of Atmospheric and Oceanic Sciences, McGill University, 805 Sherbrooke Street West, Montreal, QC H3A 2K6, Canada.

S. Brönnimann, A. M. Fischer, E. Rozanov, and M. Schraner, Institute for Atmospheric and Climate Science, ETH Zurich, CH-8092 Zürich, Switzerland. (andreas.fischer@env.ethz.ch)

G. Faluvegi and D. T. Shindell, NASA Goddard Institute for Space Studies, 2880 Broadway, New York, NY 10025, USA.